

# Shape and surface area measurements using scanning electron microscope stereo-pair images of volcanic ash particles

Owen P. Mills<sup>1</sup> and William I. Rose<sup>2</sup>

<sup>1</sup>*Materials Science and Engineering Department, Michigan Technological University, 1400 Townsend Drive, Houghton, Michigan 49931, USA*

<sup>2</sup>*Geological and Mining Engineering and Sciences Department, Michigan Technological University, 1400 Townsend Drive, Michigan 49931, USA*

## ABSTRACT

The shape and surface area of fine particles are traditionally measured using projected or two-dimensional (2D) sections or with nitrogen gas adsorption using the BET (Brunauer, Emmett, and Teller) method. However, 2D sections are incomplete shape descriptors and nitrogen gas adsorption analysis is precluded when the amount of sample is limited, for example, in direct ash cloud sampling. In this study we present a technique for measuring the shape and surface area of individual grains of volcanic ash using scanning electron microscope (SEM) stereo pairs. The application we discuss is the stereoscopic analysis of 25 ash particles in the 4–130  $\mu\text{m}$  size range from the August 1992 Crater Peak–Spurr eruption, located 130 km west of Anchorage, Alaska. Surface area data are presented from stereo measurements of glass microspheres in the same size range as validation of the technique's accuracy. Differences in surface area values between our technique, 2D shape data, and nitrogen gas adsorption are presented and discussed.

## INTRODUCTION

Volcanic eruptions inject very fine volcanic ash (<60  $\mu\text{m}$  in diameter) into the stratosphere, where it may reside for periods of hours to days. Ash fallout is directly influenced by ash morphology, i.e., size, shape, and surface complexity. Understanding morphologic factors also leads to better understanding of micro-physical processes in the cloud and reactions on particle surfaces (Durant, 2007; Rose and Durant, 2009).

The scanning electron microscope (SEM), with attributes of both large depth of field and superior resolution relative to optical light microscopy, is an excellent tool for the study of volcanic ash particle morphology, facilitat-

ing measurement of surface texture and size and shape. Until recently, projected or two-dimensional (2D) ash particle imagery has been analyzed using qualitative terminology (Heiken and Wohletz, 1985), such as vesicular, angular, blocky, subangular, and elongate. These descriptors have been successfully used to classify ash sources by geologists with experience identifying ash texture (Sheridan and Marshall, 1983), but are probably not as useful to the less practiced. It has been recognized that these qualitative descriptors do not fully characterize the complex shapes observed (Maria and Carey, 2002). Even so, most of the research into quantitative shape descriptors conducted by earth scientists has been restricted to 2D imagery. For example, research using conventional image analysis undertaken on 2D SEM ash particle imagery concluded that aspect ratio and average Feret measurements provide a quantitative shape descriptor (Riley et al., 2003; Horwell et al., 2003b). The search for a single-parameter shape identifier has led to fractal-based schemes, again using 2D information, from transmitted light optical images (Maria and Carey, 2002). Particle shape has also been described as a function of surface structure (Ersoy et al., 2007) using SEM images of pyroclast surfaces, yielding shape descriptors that include form factor, roundness, compactness, and aspect ratio. These 2D approaches ignore the overall shape of the entire particle, and in our judgment, provide an incomplete shape analysis. Increased computational speeds with low-cost computers and sophisticated point-matching algorithms have made quantitative stereo-pair analysis (3D) more accessible (Podsiadlo and Stachowiak, 1997). Recently, SEM stereo-pair analysis has been used to determine microscale roughness factors for vesicular volcanic ash particles (Carter et al., 2009) using a software program, Alicona MeX (Alicona GmbH, Graz, Austria; <http://www.alicon.com>) to extract roughness data from the image pairs.

In particular, we note that in each of these 3D studies the primary focus was characterization of surface topographies rather than entire objects. In contrast, in our study we characterize whole particle shape, including surface topography.

Characterization and quantification of surface area are important to researchers investigating both the transport (e.g., effects of particle shape on atmospheric drag; Wilson and Huang, 1979) and reactivity (respirable health effects; Horwell et al., 2003a, 2003b, 2007) of fine ash. Surface area (SA) measurements have traditionally been made with nitrogen gas adsorption technology, commonly known as the BET (Brunauer, Emmett, and Teller; Brunauer et al., 1938) method. Recent work focusing on the effects of fine ash on public health utilized this proven technique (Horwell et al., 2003a, b). Nitrogen gas adsorption analysis requires a few grams of material for measurement, a reasonable possibility when sufficient deposits are available. However, this requirement precludes the use of nitrogen gas adsorption analysis where samples are limited to small volumes, for example, direct ash sampling exercises (Horwell et al., 2003b).

Here we describe a technique using SEM stereo pairs and 3D software, MeX, for simultaneous measurement of shape and surface area of individual fine volcanic ash particles from the August 1992 Crater Peak–Spurr eruption. Crater Peak, on the southern flank of Mount Spurr, is located 130 km west of Anchorage, Alaska. The eruption of 18 August 1992 ejected andesitic material to a height of 14 km above sea level. The sample used in the study, Ashton 57, was collected 275 km southeast of the volcano (McGimsey et al., 2001).

## MATERIALS AND METHODS

SEM samples were prepared by dispersing ash onto carbon adhesive-coated aluminum SEM mounts. The adhesive-coated aluminum mount

is placed beside ~0.25 g of ash in a plastic cup and sealed with a lid. A single perforation in the lid accommodates entry of the tube from a cylinder of compressed air. A short burst of air floats the ash inside the sealed cup and ash particles settle onto the adhesive-coated mount (Scott Wight, National Institute of Standards and Technology, 2009, personal commun.). The samples were carbon coated with a tilted rotating carousel to ensure electric conduction to the mount and to reduce sample charging. A representative SEM image of volcanic ash prepared in this manner, exhibiting complex shapes and a wide range of size, is presented in Figure 1.

Secondary electron stereo-pair images of individual particles were taken using a JEOL 6400 SEM (JEOL, USA, Inc., Peabody, Massachusetts) equipped with a Geller MicroAnalytical dPict digital image acquisition system (Geller MicroAnalytical Laboratory, Inc., Topsfield, Massachusetts). SEM operational parameters were 20kV accelerating voltage, 15 mm working distance, and stage tilt angles of 8°. A beam current of 0.45 nA was used. A stereo pair for a particle used in this work is shown in Figure 2. We used 1000 × 750 pixel images because high pixel density is critical to the quality of stereo-

pair results. The SEM has a resolution estimated at 10 nm, or 400 times smaller than the smallest particles we studied; this suggests that the SEM can map all but the finest-scale roughness of such particles.

Herein we compare our 3D surface area and volume measurements with 2D area results of Riley et al. (2003), who employed 2D image analysis software to produce a selection of size and shape results; a brief explanation of area estimates made using that technique is warranted. Image analysis-based 2D surface area estimates are produced using an edge detection algorithm that sifts through pixels in the projected image and identifies the perimeter as a change in contrast between the particle and the adjoining background (Fig. 3). The enclosed area is obtained when filled with pixels whose size is calibrated to the image scale.

The 3D measurements of surface area and volume were made with the MeX software program. The SEM image pair was read into the MeX Stereo Creator software module and points in both images, belonging to a single point on the specimen surface, were identified by changes in specimen surface texture. The z-axis coordinate of the feature is generated by the MeX software with operator-supplied SEM

parameters that include tilt angle, the distance between the specimen surface and the final lens (working distance), and calibrated pixel size. This process is repeated for each pixel in the image pair to form a digital elevation model (DEM) (Fig. 4). We note that the DEM is essentially a 3D topographic relief map of the specimen surface. The perimeter of an ash particle is delineated by manually outlining the particle using the MeX area analysis module. Data from the third dimension were analyzed at the intersections of a grid superimposed on the DEM data set that delineates z-axis profiles used to estimate area and volume. The selected area is converted to 3D surface area and volume estimates based on proprietary calculations used in the MeX software. The basic 3D calculations were described in Boyde (1973). A computerized point-matching scheme was described in Podsiadlo et al. (1997). The total time required for the 3D analysis with MeX is ~15 min. That estimate includes the time required to collect a pair of digital images, load the files into MeX, process a DEM, and measure the surface area and volume. The elapsed time is highly dependent on the computer configuration. We currently use a personal computer with a 3 GHz Intel Core 2 Duo (Intel Inc., Santa Clara, California,

**Figure 1.** Volcanic ash sample examined for this paper. Ash has a wide range of sizes and each particle exhibits a complex shape, as shown by scanning electron microscope images of bulk sample of distal 19 August 1992 ashfall from Crater Peak, Mount Spurr, Alaska (Riley et al., 2003).

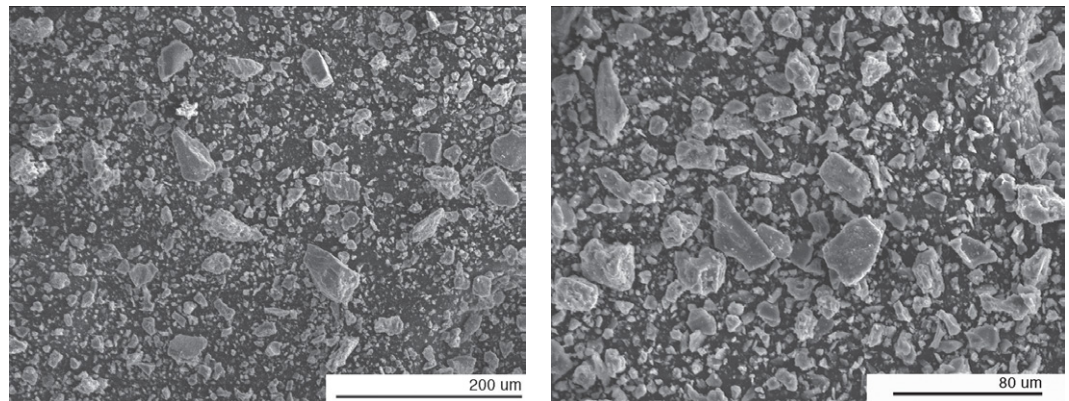
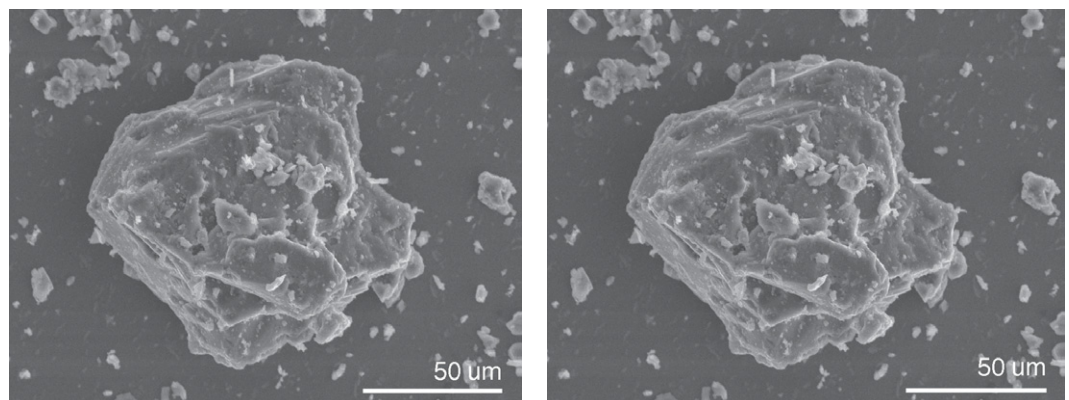


**Figure 2.** Scanning electron microscope stereo pair of a single Spurr pyroclast, taken at 8° tilt angle, found to be optimal for developing a digital elevation model and the particle shape. This image is particle 20 in Table 1.



## Shape and surface area measurements

**Figure 3.** Visual comparison of surface area analysis methods for particle 11 (Table 1). (A) For two-dimensional image, surface area,  $SA = 1082 \mu\text{m}^2$ . (B) For a three-dimensional (3D) image,  $SA = 1617 \mu\text{m}^2$ . Here, the 3D surface area from Table 1 has been halved so that upper surface areas are compared in both cases. The 3D-based SA estimate is markedly higher than the perimeter-based 2D estimate.

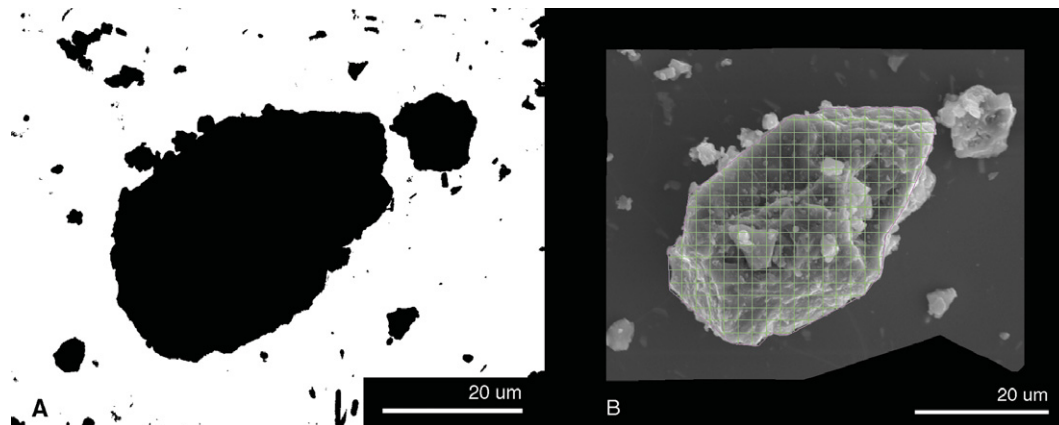
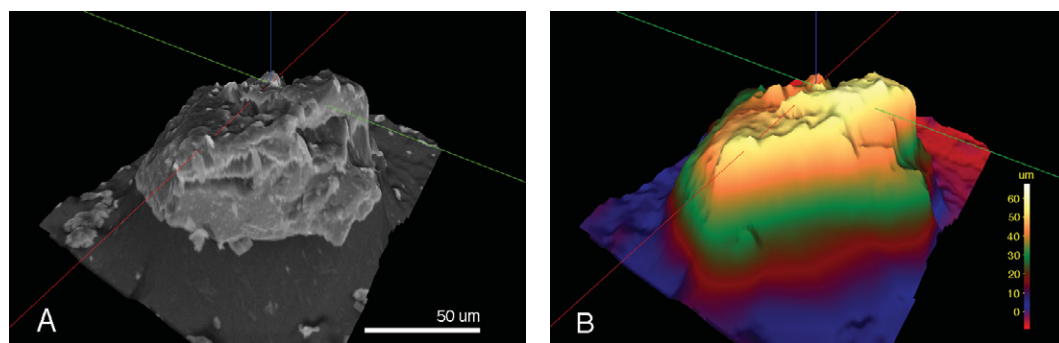


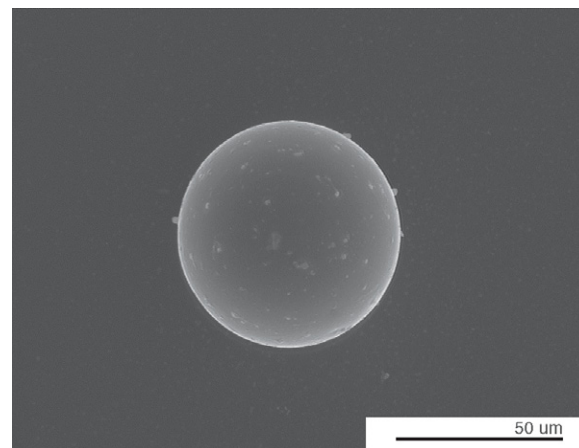
**Figure 4.** Two views of digital elevation model produced from stereo pair in Figure 2, using MeX software (see text) ([www.alicon.com](http://www.alicon.com)). (A) Grayscale shaded relief map. (B) Colored height contour map.



[www.Intel.com](http://www.Intel.com)) microprocessor, 3 GB of memory, and a high performance video card with 512 MB of memory.

Identically prepared precision glass microspheres (Duke Scientific, Fremont, California, [www.dukescientific.com](http://www.dukescientific.com)) were measured using MeX to serve as a validation of the technique. MeX 3D reconstruction requires reference points on the specimen surface resulting from textural changes. DEMs of the spheres and the resulting area and volume measurements are only possible due to the ultrafine particles that we found dispersed on the otherwise smooth glass microspheres (Fig. 5). These nanometer-scale particles were found on all microspheres in varied surface distributions. Subject microspheres with an even coating of fine particles were chosen to produce high-quality DEMs. We note that the glass microspheres do not resemble complex ash shapes. However, we know of no other suitable test specimen that is both uniform in shape and whose shape can be mathematically reproduced. Furthermore, the glass spheres can be obtained in different size ranges. The surface area of the glass microspheres, determined based on 3D SEM images, agreed within 10% of their calculated area (Fig. 6), affirming the ability of the technique to generate accurate results in this geometrically

**Figure 5.** Scanning electron microscope image of glass microsphere used in MeX validation (<http://www.alicon.com>). Specimen surface texture is required for accurate digital elevation models (DEMs). The ultrafine particles dispersed on the otherwise smooth glass spheres make DEMs possible. This image is microsphere 14 in Table 1.



simple circumstance. We do not have access to the lower surface of the ash particles or microspheres and therefore assume that the lower surface is similar to the upper. We presume that ash from a particular eruptive event will have similar composition and density and that individual particles will exhibit similar shape characteristics. We did not observe spherical distortion in the microspheres and therefore have no reason to suspect deviation between theoretical and measured surface areas.

Nitrogen gas adsorption data were collected with a Micromeritics ASAP 2000 system (Norcross, Georgia, [www.micromeritics.com](http://www.micromeritics.com)). We evaluated the accuracy of those measurements utilizing a silica glass surface area reference material obtained from the equipment manufacturer. In tests using our instrument, we generated results that placed the Micromeritics reference material surface area result at  $4.91 \text{ m}^2/\text{g}$ . This result compares favorably with the manufacturers specified determination of  $4.8 \pm 0.3 \text{ m}^2/\text{g}$ .



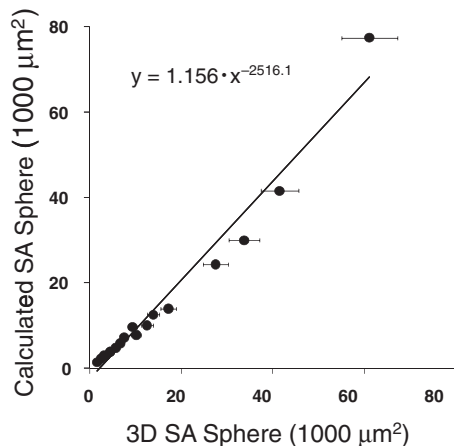


**Figure 6.** Stereo scanning electron microscope three-dimensional (3D) measurements of microsphere surface area plotted with theoretical surface area (SA) of spheres with variable diameters. The plot demonstrates expected agreement, as a majority of the 3D measured surface areas are within the 10% of the calculated surface area errors.

**RESULTS AND DISCUSSION**

We selected 25 ash particles from the Crater Peak–Spurr fallout ranging in size from 4 to 130 μm and determined selected characteristics with MeX. The particles chosen for study were selected from a heterogeneous population of ash particles on the SEM sample mount. Subject particles were randomly chosen from low magnification images of that mount. Particles selected were then used to make stereo-pair images at higher magnification. No effort was made to classify particles during the selection process. This method represents a departure from other studies on ash, where bulk samples were separated by size (Sheridan and Marshall, 1983) or terminal velocity (Wilson and Huang, 1979; Riley et al., 2003) prior to classification. We present 3D surface area and volume data and compare that to published 2D values. The 2D data set was produced by Riley et al. (2003) using image analysis of projected SEM images of the same Spurr ash sample used in the work. The 3D data set was created from a pair of projected images tilted 8° with respect to each other and processed with MeX software into a DEM (details shown in Table 1).

**Shape**

Because the shape and surface area of a particle are inextricably linked, any discussion of particle shape must necessarily involve surface

**TABLE 1.** STEREO SEM-BASED ESTIMATES OF THE SURFACE AREAS OF 25 PARTICLES FROM CRATER PEAK–SPURR DISTAL FALL OF 19 AUGUST 1992 AND FROM GLASS MICROSPHERES OF VARIOUS SIZES USING MEX SOFTWARE

| Particle | Ash particles |                          |  |
|----------|---------------|--------------------------|--|
|          | CED (μm)      | SA 3D (μm <sup>2</sup> ) | SA = 4π(CED/2) <sup>2</sup> (μm <sup>2</sup> ) |
| 1        | 4             | 36                       | 48   |
| 2        | 5             | 48                       | 76   |
| 3        | 6             | 82                       | 96   |
| 4        | 6             | 80                       | 96   |
| 5        | 8             | 162                      | 192  |
| 6        | 12            | 364                      | 440  |
| 7        | 15            | 412                      | 676  |
| 8        | 15            | 702                      | 748  |
| 9        | 19            | 1312                     | 1148   |
| 10       | 23            | 2234                     | 1724   |
| 11       | 34            | 3234                     | 3720   |
| 12       | 40            | 4616                     | 4928   |
| 13       | 42            | 4450                     | 5548   |
| 14       | 61            | 7850                     | 11864  |
| 15       | 66            | 10998                    | 13616  |
| 16       | 66            | 11072                    | 13744  |
| 17       | 74            | 13844                    | 17252  |
| 18       | 76            | 17462                    | 18200  |
| 19       | 84            | 23376                    | 22284  |
| 20       | 103           | 31662                    | 33212  |
| 21       | 105           | 34264                    | 34592  |
| 22       | 118           | 44638                    | 43600  |
| 23       | 123           | 44842                    | 47212  |
| 24       | 124           | 38962                    | 48148  |
| 25       | 130           | 52124                    | 53132  |

| Particle | Glass microspheres |                          |  |
|----------|--------------------|--------------------------|--|
|          | Diameter (μm)      | SA 3D (μm <sup>2</sup> ) | SA = 4π(CED/2) <sup>2</sup> (μm <sup>2</sup> ) |
| 1        | 21.0               | 1650.1                   | 1385.4   |
| 2        | 26.9               | 2451.9                   | 2273.3   |
| 3        | 30.5               | 3386.8                   | 2912.9   |
| 4        | 31.1               | 3060.2                   | 3036.6   |
| 5        | 34.9               | 4430.2                   | 3830.9   |
| 6        | 35.2               | 4499.6                   | 3881.5   |
| 7        | 38.9               | 5630.5                   | 4746.6   |
| 8        | 42.9               | 6682.0                   | 5789.9   |
| 9        | 47.8               | 7459.0                   | 7163.0   |
| 10       | 49.9               | 10123.2                  | 7825.8   |
| 11       | 55.5               | 9341.7                   | 9669.9   |
| 12       | 56.5               | 12496.1                  | 10039.4  |
| 13       | 63.2               | 13873.2                  | 12528.5  |
| 14       | 66.6               | 17148.6                  | 13922.2  |
| 15       | 88.0               | 27481.0                  | 24345.1  |
| 16       | 97.7               | 33735.2                  | 29987.5  |
| 17       | 115.0              | 41506.0                  | 41547.7  |
| 18       | 157.0              | 61152.4                  | 77437.3  |

*Note:* Both lists are in ascending order of diameters. 3D—three-dimensional; SEM—scanning electron microscope; CED—circle of equivalent diameter; SA—surface area. MeX software: Alicona GmbH, Graz, Austria ([www.alicon.com](http://www.alicon.com)).

area. The relationship between surface area and volume for individual particles, expressed as a ratio (SA/V), is a tool useful in characterizing the shape of the small, complex-shaped particles observed in fine volcanic ash. The theoretical 2D surface area and volume can be calculated using a circle of equivalent diameter (CED, in μm), a factor defined as the diameter of a circle with an area equivalent to that of the irregular object

$$CED = 2 \left( \frac{area}{\pi} \right)^{1/2}, \quad (1)$$

where area (μm<sup>2</sup>), in this instance, is from the Riley et al. (2003) data set. Surface area (SA, in μm<sup>2</sup>) may be estimated from a 2D image using the relationship

$$SA = 4\pi \left( \frac{CED}{2} \right)^2. \quad (2)$$

Likewise, volume (V, in μm<sup>3</sup>) is estimated from 2D images using

$$V = \frac{4}{3} \pi \left( \frac{CED}{2} \right)^3. \quad (3)$$

Shape and surface area measurements

Although the CED approximation is commonly reported in 2D particle studies (Riley et al., 2003), it should be recognized that use of the CED will misrepresent the true surface area, leading to an error that scales with particle shape complexity. Because additional shape data are provided from 3D measurements, we expect 3D SA/V ratios to be greater than those calculated from 2D estimates. The 3D-derived SA/V ratio is greater than 2D SA/V ratio by factors of 1.4 and 2.1 for particle sizes of 4 μm and 130 μm, respectively (Fig. 7). Note that the 2D-derived estimates are based on many particles from a common terminal velocity group (Riley et al., 2003), while the 3D estimate is for a single particle.

Two-dimensional imagery, using aspect ratio measurements of particle axes, may be applied to calculate a shape factor (Wilson and Huang, 1979; Riley et al., 2003). The shape factor, SF, described by Wilson and Huang (1979), is  $SF = (b + c)/2a$ , where a, b, and c correspond to caliper measurements of the long, intermediate, and short axes, respectively. The calculation yields a factor of 0.8 for Spurr ash (Riley

et al., 2003). A shape factor, λ, for a nonspherical particle has also been developed (e.g., that of Geiger and Poirier, 1973):

$$\lambda = \left( \frac{SA}{V} \right) \left( \frac{D_p}{6} \right), \quad (4)$$

where  $D_p$  (in μm) is a characteristic dimension of the irregular particle. Utilizing the SA/V ratio from their equation, we compare 3D SA/V values for individual Spurr ash particles determined in this study with MeX to SA/V values calculated from an equivalent spherical diameter (ESD, in μm). The equivalent spherical diameter of an irregular particle expresses the diameter of a sphere with equal volume

$$ESD = 2 \left( \frac{3V}{4\pi} \right)^{1/3}, \quad (5)$$

where V is MeX-measured volume. The Spurr 3D SA/V data presented here in Figure 8 were measured with MeX software. In this case, SA and V are equivalent to the expressions developed as equations 2 and 3 after replacing CED with ESD. Observed differences between 3D and data points calculated using a spherical diameter, ESD (Fig. 8), are systematic but expected, and indicative of particle complexity, i.e., the SA/V ratio increases with decreasing particle size. The 3D SA/V estimates exceed the ESD calculated SA/V ratio by factors of 1.5 and 1.9 at particle sizes of 4 μm and 130 μm, respectively. Thus, development of a single factor describing particle shape is problematic.

Note that accessibility to the surface area of individual particles is facilitated by 3D stereo-pair analysis and this shape factor calculation may be done on a particle by particle basis.

Although there is a clear relationship between SA/V and particle size and complexity, there is also some degree of scatter (Figs. 7 and 8) imparted when the sample size is expanded from a single particle (3D analysis) to a population of particles (2D analysis; Riley et al., 2003). It is possible that MeX may not accurately estimate surface area and volume for all particle shapes and orientations depending on particle aspect ratio and orientation on the SEM mount. More measurements of the same particles with different geometric positions within the SEM could test MeX inaccuracies much more thoroughly, but we did not do this.

Sources of uncertainty reported in figures and tables include that associated with the manufacturer calibrations of the SEM scale and with manual tracing of the particle perimeter in MeX and 2D image analysis error. The manufacturer-specified difference between reference images and the scale bar is estimated to be <2%. The coefficient of variation for multiple tracings (n = 10) of particle perimeter using MeX software is 0.02% (CED = 3.9 μm, 42 μm, and 130 μm). The error from the two sources, extended through the entire calculation, is not reproduced explicitly in the figures. We do not have access to the raw data of Riley et al. (2003) and are therefore unable to quantify image analysis error associated with their 2D measurements.

Surface Area

The measurement of nitrogen gas adsorption on surfaces of a bulk sample of fine particles provides an independent method for the determination of particle surface area and has been applied to samples of volcanic ash (Riley et al., 2003; Horwell et al., 2003a; Delmelle et al., 2005). Nitrogen gas adsorption surface area is reported as a single value for a sample composed of particles with variable diameters. Because SA/V is higher for finer particles, fines strongly influence estimates of bulk surface area.

A nitrogen gas adsorption measurement for our Spurr ash sample yielded a surface area value of 1.71 m<sup>2</sup>/g (Table 2). We sought to reconcile the nitrogen gas adsorption surface area, determined for a bulk sample, with those obtained for individual particles. The calculations involved in this comparison utilize the Spurr particle size distribution (PSD) of Riley et al. (2003) and MeX surface area and volume measurements for individual particles of variable size. The PSD of the bulk samples was measured by laser diffraction using a Malvern Mastersizer instrument

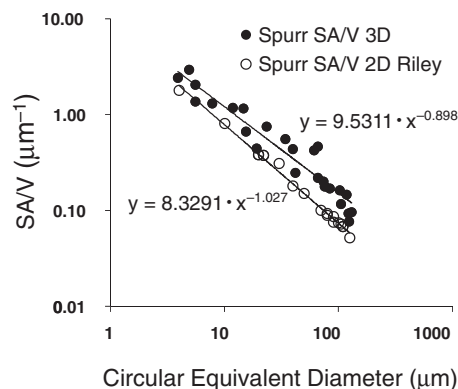


Figure 7. Plot of data from surface area/volume (SA/V) relationships determined from two-dimensional (2D) and 3D data. The 2D method uses SA and V data calculated on their circular equivalent diameter determined from scanning electron microscope (SEM) images (Fig. 3) by Riley et al. (2003). The 2D data are based on many particles with the same terminal velocities. The 3D data plotted are based on values determined from only one particle using SEM stereo pairs and MeX software (<http://www.alicon.com/>), as shown in Figure 3. The figure shows that 3D measurements give greater SA/V estimates by factors of 1.4–2.1. This is expected because spherical-based assumptions are violated by real ash particles.

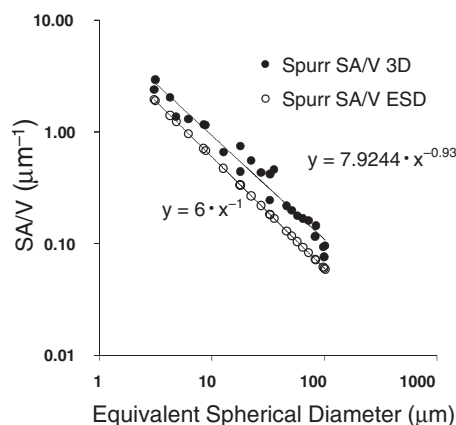


Figure 8. Surface area/volume (SA/V) plot, as in Figure 7, comparing 3D volcanic ash surface areas to spherical surface areas calculated with equivalent spherical diameters. Data are from Table 1. The plot shows that the three-dimensional SA/V ratio exceeds the equivalent spherical diameter-derived SA/V ratio by factors of 1.5–1.9.

(Table 3). Surface area was estimated from SEM stereo pairs of ash particles using MeX software, as described herein. Volume percent data from the PSD were calculated for each binned particle size in the 0–130  $\mu\text{m}$  range. An average SA/mass ratio was calculated for every 10- $\mu\text{m}$ -diameter group using the MeX surface area and volume. An ash density of 1900  $\text{kg}/\text{m}^3$  was used in the mass calculation. The mass/volume results were totaled and normalized to the volume fraction grouping for comparison to the bulk surface area derived from nitrogen gas adsorption analysis. MeX 3D surface area and volume values are used in the calculation to estimate bulk surface area for the microspheres. All steps were the same except that the mass calculation for microspheres used the manufacturer-specified density of 2550  $\text{kg}/\text{m}^3$ .

The results obtained here (Table 2) yielded an MeX-measured surface area 43% greater than that reported by Riley et al. (2003; 2D results) and 8.5 times less than our nitrogen gas adsorption-derived value, the latter factor being comparable to that determined by Riley et al. (2003). We suspect that the greater surface area resulting from application of the nitrogen gas adsorption approach results from two factors: (1) exclusion of surface area data in the 0.02–4  $\mu\text{m}$  range and (2) irresolvable microporosity effects. We determined surface area of particles in the 4–130  $\mu\text{m}$  size range with MeX, yet the PSD shows that 10.6% of the particles ranged between 0.02 and 4  $\mu\text{m}$ . Finer particles have greater surface areas relative to volume, and exclusion of even a small volume fraction can contribute to a significant difference in estimated surface area. In a detailed nitrogen gas adsorption study of volcanic ash, Delmelle et al. (2005) concluded that micropores of ~5 nm were present and contributed to the true surface area. Features of this size, whether the result of porosity or surface roughness, are not resolved in the SEM used in this study. This is especially true given the 500–15,000 times magnifications we used to image entire particles. A feature will be recognized and therefore included in the MeX surface area results if it is resolved in the SEM images, a condition that is limited by the diameter of the SEM electron beam. The manufacturer-specified resolution for the SEM used in this research is 10 nm. A resolution of 2.5 nm is required to reliably resolve features of 5 nm. The secondary electrons used to form the SEM image are generated at depths as great as 50 nm within the sample surface, and geometric constraints, such as holes, may limit detection or even prevent the signal from reaching the detector. This would be the case for the 5 nm micropores noted by Delmelle et al. (2005), and these features would not be observed in the images or preserved in the MeX surface area results.

TABLE 2. SUMMARY OF SURFACE AREA ESTIMATES MADE WITH DIFFERENT METHODS FOR AN ASH SAMPLE FROM CRATER PEAK–SPURR AND MICROSPHERES

|  | Crater Peak–Spurr | Microsphere |
|--|-------------------|-------------|
| 1. 3D $\text{m}^2/\text{g}$ (MeX)                | 0.20              | 0.04        |
| 2. 2D $\text{m}^2/\text{g}$ (Riley et al., 2003) | 0.14              | NA          |
| 3. Nitrogen gas adsorption $\text{m}^2/\text{g}$ | 1.71              | 0.12        |

Note: Row 1: Bulk surface area estimates for the ash calculated from MeX data (MeX software: Alicona GmbH, Graz, Austria [www.alicon.com]) and grain-size laser diffraction data of the ash and microspheres. 3D—three-dimensional. Row 2: 2D estimates based on perimeter data determined by Riley et al. (2003) and the grain-size data. Row 3: Results from bulk nitrogen gas adsorption measurements of ash and microspheres. Note that nitrogen gas adsorption estimates of surface areas are significantly higher (see text for discussion). NA—not analyzed.

TABLE 3. PARTICLE SIZE DISTRIBUTION OF THE CRATER PEAK/SPURR ASH SAMPLE MEASURED WITH LASER DIFFRACTION INSTRUMENTATION\*

| Particle size ( $\mu\text{m}$ ) | Volume (%) | Particle size ( $\mu\text{m}$ ) | Volume (%) |
|---------------------------------|------------|---------------------------------|------------|
| 0.020                           | 0.00       | 7.096                           | 1.80       |
| 0.022                           | 0.00       | 7.962                           | 1.96       |
| 0.025                           | 0.00       | 8.934                           | 2.19       |
| 0.028                           | 0.00       | 10.024                          | 2.40       |
| 0.032                           | 0.00       | 11.247                          | 2.63       |
| 0.036                           | 0.00       | 12.619                          | 2.85       |
| 0.040                           | 0.00       | 14.159                          | 3.04       |
| 0.045                           | 0.00       | 15.887                          | 3.19       |
| 0.050                           | 0.00       | 17.825                          | 3.29       |
| 0.056                           | 0.00       | 20.000                          | 3.32       |
| 0.063                           | 0.00       | 22.440                          | 3.28       |
| 0.071                           | 0.00       | 25.179                          | 3.19       |
| 0.089                           | 0.00       | 28.251                          | 3.05       |
| 0.100                           | 0.00       | 31.698                          | 2.91       |
| 0.112                           | 0.00       | 35.566                          | 2.78       |
| 0.126                           | 0.00       | 39.905                          | 2.71       |
| 0.142                           | 0.00       | 44.774                          | 2.71       |
| 0.159                           | 0.00       | 50.238                          | 2.79       |
| 0.178                           | 0.00       | 56.368                          | 2.94       |
| 0.200                           | 0.00       | 63.246                          | 3.14       |
| 0.224                           | 0.00       | 70.963                          | 3.35       |
| 0.252                           | 0.00       | 79.261                          | 3.50       |
| 0.283                           | 0.00       | 89.337                          | 3.56       |
| 0.317                           | 0.00       | 100.237                         | 3.49       |
| 0.356                           | 0.00       | 112.468                         | 3.27       |
| 0.399                           | 0.00       | 126.191                         | 2.91       |
| 0.448                           | 0.04       | 141.589                         | 2.45       |
| 0.502                           | 0.09       | 158.866                         | 1.93       |
| 0.564                           | 0.17       | 178.250                         | 1.40       |
| 0.632                           | 0.22       | 200.000                         | 0.90       |
| 0.710                           | 0.27       | 224.404                         | 0.52       |
| 0.796                           | 0.31       | 251.785                         | 0.11       |
| 0.893                           | 0.34       | 282.508                         | 0.00       |
| 1.002                           | 0.36       | 316.979                         | 0.00       |
| 1.125                           | 0.39       | 355.656                         | 0.00       |
| 1.262                           | 0.43       | 399.052                         | 0.00       |
| 1.416                           | 0.47       | 447.744                         | 0.00       |
| 1.589                           | 0.52       | 502.377                         | 0.00       |
| 1.783                           | 0.59       | 563.677                         | 0.00       |
| 2.000                           | 0.66       | 632.456                         | 0.00       |
| 2.244                           | 0.74       | 709.627                         | 0.00       |
| 2.518                           | 0.82       | 796.214                         | 0.00       |
| 2.825                           | 0.91       | 893.367                         | 0.00       |
| 3.170                           | 1.00       | 1002.374                        | 0.00       |
| 3.557                           | 1.09       | 1124.683                        | 0.00       |
| 3.991                           | 1.18       | 1261.915                        | 0.00       |
| 4.477                           | 1.28       | 1415.892                        | 0.00       |
| 5.024                           | 1.39       | 1588.656                        | 0.00       |
| 5.637                           | 1.51       | 1782.502                        | 0.00       |
| 6.325                           | 1.64       | 2000.000                        | 0.00       |

\*Data of Riley et al. (2003).

## SUMMARY AND CONCLUSIONS

In this work we demonstrate that particle surface area and volume values derived from 3D SEM stereo-pair analysis can be used to objectively identify ash particle shape. Using this technique, we assimilate particle surface area data into a single surface area value comparable to that derived from nitrogen gas adsorption measurements. The analysis was carried out on 25 ash particles in the range 4–130  $\mu\text{m}$  collected from the 19 August 1992 Crater Peak–Spurr eruption.

Stereo pairs, taken from SEM digital images, were processed using the 3D analysis software package MeX. MeX output includes DEMs, but additionally provides surface area and volume values from the processed SEM images. All of the information we present was acquired only from the upper particle surface, i.e., the lower surface is obscured and assumed to have characteristics resembling that of the upper surface. The 3D results were validated using stereo-pair images of glass microspheres acquired under the same conditions.

We have applied SA/V ratio analysis to volcanic particles in the search for an objective shape descriptor. Ash particle shape can be characterized using surface area measured from a single particle with SEM stereo-pair images. A ratio, SA/V, has been developed that shows promise as a shape descriptor that does not rely on the qualitative shape determinations typically utilized with 2D images. The SA/V ratio increases as particle size decreases. Owing to the additional surface area information accessible with 3D imagery, we were able to demonstrate that 3D SA/V ratios may be as much as 2.1 times greater than those obtained from 2D surface area results and 1.5–1.9 times greater than those calculated using equivalent spherical diameter. Morphological shape determinations are frequently carried out in the SEM, and we believe that the enhanced surface area data available through application of this technique offsets the additional time required to acquire and process the two stereo images. Assessing the general applicability of the SA/V ratio as a

quantitative shape descriptor will be aided by analysis of a greater number of samples with attention to whether the ratio will discriminate particles from different types of deposits.

The individual MeX 3D surface area information used in the particle shape portion of this study was recast into a single bulk sample value using laser diffraction particle size information, permitting comparison to nitrogen gas adsorption data for ash and glass microspheres. The resulting nitrogen gas adsorption surface area value for ash was 8 times greater than the amalgam of single particle data but only a factor of 3 greater for microspheres. This disparity can be attributed to the exclusion of very fine particles from the SEM-based technique and the occurrence of microporosity in the ash that is not present in glass microspheres. The 3D surface area SEM measurements such as those in this paper could be advantageous when sample size is limited, such as aircraft ash sampling exercises (Horwell et al., 2003b).

The 3D SEM stereo imaging technique presented here provides a novel way to use particle surface area to characterize particle shape, and in some situations, provides a substitute for nitrogen gas adsorption analysis. The stereo-imaging technique is laborious compared to 2D image analysis and would therefore be most attractive where only small amounts of sample are available.

## ACKNOWLEDGMENTS

We thank S.A. Hackney, M.T. Auer, and A.J. Durant for their advice and critical review of this work.

## REFERENCES CITED

- Boyd, A., 1973, Quantitative photogrammetric analysis and qualitative stereoscopic analysis of SEM images: *Journal of Microscopy*, v. 93, no. 3, p. 452–471.
- Brunauer, S., Emmett, P.H., and Teller, E., 1938, Adsorption of gases in multimolecular layers: *American Chemical Society Journal*, v. 60, p. 309–319, doi: 10.1021/ja01269a023.
- Carter, A., Ramsey, M., Durant, A., and Skilling, I., 2009, Micron-scale roughness of volcanic surface from thermal infrared spectroscopy and scanning electron microscopy: *Journal of Geophysical Research*, v. 114, B02213, doi: 10.1029/2008JB005632.
- Delmelle, P., Villeras, F., and Pelletier, M., 2005, Surface area, porosity and water adsorption properties of fine volcanic ash particles: *Bulletin of Volcanology*, v. 67, p. 160–169, doi: 10.1007/s00445-004-0370-x.
- Durant, A.J., 2007, On water in volcanic clouds [Ph.D. thesis]: Houghton, Michigan Technological University, 242 p.
- Ersoy, O., Gourgaud, A., Aydar, E., Chinga, G., and Thouret, J.C., 2007, Quantitative scanning-electron microscope analysis of volcanic ash surfaces: Application to the 1982–1983 Galunggung eruption (Indonesia): *Geological Society of America Bulletin*, v. 119, p. 743–752, doi: 10.1130/B26048.1.
- Geiger, G.H., and Poirier, D.R., 1973, *Transport phenomena in metallurgy*: Reading, Massachusetts, Addison-Wesley, 616 p.
- Heiken, G., and Wohletz, K., 1985, *Volcanic ash*: Berkeley, University of California Press, 246 p.
- Horwell, C.J., Fenoglio, I., Ragnarsdottir, K.V., Sparks, R.S.J., and Fubini, B., 2003a, Surface reactivity of volcanic ash from the eruption of Soufriere Hills volcano, Montserrat, West Indies with implications for health hazards: *Environmental Research*, v. 93, p. 202–215, doi: 10.1016/S0013-9351(03)00044-6.
- Horwell, C.J., Sparks, R.S.J., Brewer, T.S., Llewellyn, E.W., and Williamson, B.J., 2003b, Characterization of respirable volcanic ash from the Soufriere Hills volcano, Montserrat, with implications for human health hazards: *Bulletin of Volcanology*, v. 65, p. 346–362, doi: 10.1007/s00445-002-0266-6.
- Horwell, C.J., Fenoglio, I., and Fubini, B., 2007, Iron-induced hydroxyl radical generation from basaltic volcanic ash: *Earth and Planetary Science Letters*, v. 261, p. 662–669, doi: 10.1016/j.epsl.2007.07.032.
- Maria, A., and Carey, S., 2002, Using fractal analysis to quantitatively characterize the shapes of volcanic particles: *Journal of Geophysical Research*, v. 107, no. B11, 2283, doi: 10.1029/2001JB000822.
- McGimsey, R.G., Neal, C.A., Riley, C.M., 2001, Areal distribution, thickness, mass, volume and grain size of tephra-fall deposits from the 1992 eruptions of Crater Peak vent, Mt. Spurr, Alaska: U.S. Geological Survey Open-File Report OF01–0370, 38 p.
- Podsiadlo, P., and Stachowiak, G.W., 1997, Characterization of surface topography of wear particles by SEM stereoscopy: *Wear*, v. 206, p. 39–52, doi: 10.1016/S0043-1648(96)07324-3.
- Riley, C.M., Rose, W.I., and Bluth, G.J.S., 2003, Quantitative shape measurements of distal volcanic ash: *Journal of Geophysical Research*, v. 108, no. B10, 2504, doi: 10.1029/2001JB000818.
- Rose, W.I., and Durant, A.J., 2009, Fine ash content of explosive eruptions: *Journal of Volcanology and Geothermal Research*, v. 186, p. 32–39, doi: 10.1016/j.jvolgeores.2009.01.010.
- Sheridan, M.F., and Marshall, J.R., 1983, Interpretation of pyroclast surface features using SEM images: *Journal of Volcanology and Geothermal Research*, v. 16, p. 153–159, doi: 10.1016/0377-0273(83)90088-4.
- Wilson, L., and Huang, T.C., 1979, Influence of shape on the atmospheric settling velocity of volcanic ash particles: *Earth and Planetary Science Letters*, v. 44, p. 311–324, doi: 10.1016/0012-821X(79)90179-1.

MANUSCRIPT RECEIVED 30 OCTOBER 2009

REVISED MANUSCRIPT RECEIVED 17 APRIL 2010

MANUSCRIPT ACCEPTED 4 MAY 2010